Acta Mech 201, 249–267 (2008)
DOI 10.1007/s00707-008-0062-2

F. Ziegler

Special design of tuned liquid column-gas dampers for the control of spatial structural vibrations

Dedicated to Professor Wilhelm Schneider on the occasion of his 70th birthday

Received: 22 January 2008 / Published online: 9 August 2008
© Springer-Verlag 2008

Abstract The relevant low-frequency modes of plan-asymmetric tall buildings and those of bridges consist of coupled translational and torsional motions. We consider the locations of the modal centers of velocity of either the rigidly assumed floors or of the bridge cross-sections to be crucial for selecting the design and the "optimal" position of the liquid absorbers. Such a tuned liquid column-gas damper, TLCGD consists of a sealed rigid piping system that is partially filled with liquid (preferably water), whose dynamics can be derived using the nonstationary Bernoulli equation properly extended to account for the relative streamline in a moving reference system. Although both the construction and working principle of TLCGDs differ from tuned mass dampers (TMD), a geometric analogy exists between these absorber types. Consequently, in a first step modal tuning is performed by means of a transformation of the TMD optimal parameters, e.g., of the Den Hartog formulas, possibly followed in a second step by fine-tuning in state-space. Such a U- or V-shaped sealed liquid column-gas damper, i.e., with the gas-spring effect taken into account, is found suitable for applications in moderately plan-asymmetric buildings (the floors' modal center of velocity falls outside of the floor plan) and for bridges with dominant horizontal vibrations. The novel design of a torsional sealed liquid column-gas damper, TTLCGD, turns out to have even higher efficiency in effectively damping strongly asymmetric buildings, where the floors' modal centers of velocity lie inside of the floor plan: in that case of an alternative design, the mid-plane of the U-shaped TLCGD is bent to a cylindrical surface that might be "nearly closed" such that the trace in the floor becomes approximately a loop. For bridges with dominating vertical flexural vibrations, a novel pipe-in-pipe design of the VTLCGD provides the vertical control force rendering the additional efficient damping. The evident features of TLCGDs are no moving mechanical parts, cheap and easy implementation into civil engineering structures, simple modification of the natural frequency and even of the damping properties, low maintenance costs, little additional weight in those cases where a water reservoir is required, e.g., for the sake of fire fighting, and with a performance comparable to that of TMDs of the spring-mass- (or pendulum-)-dashpot type.

1 Introduction

Slender and lightweight civil engineering structures have rather low structural damping and thus are prone to vibrations under dynamic loads like earthquakes and various kinds of wind excitations, as well as under traffic loads, especially when acting on bridges. In many cases, an increased effective structural damping suffices to keep the dynamic response within the allowable elastic limits. Since the direct application of damping devices (of viscous or frictional nature) suffers from the low values of the displacement gradients, tuned

F. Ziegler (✉)
Institute of Building Construction and Technology, Vienna University of Technology, 1040/E2063 Vienna, Austria
E-mail: franz.ziegler@tuwien.ac.at
Fax: +43-1-5880120199

mechanical dampers (TMD) are commonly used to remove and dissipate kinetic energy in a concentrated manner from the vibrating main structure. Such TMDs are either of the spring-mass-dashpot type, Petersen [1], or rely on a pendulum-dashpot system. Moving mechanical parts can be saved at all with minimum construction and maintenance costs, by substituting the TMD by an (equivalent) tuned liquid column-gas damper, TLCGD, recently invented by Hochrainer [2], see also [3] for the analogy to TMD-tuning and [4] for mitigation of wind- and earthquake excited vibrations of tall buildings with in-plane (horizontal) translational natural modes. The gas-spring effect inherent in this sealed design of U- or V-shaped liquid absorbers allows simple tuning of the eigen-frequency in an even extended range of "low frequencies". The optimal damping coefficient relies on viscous and turbulent fluid damping causing the required energy dissipation and since it is less accessible needs to be assigned by prior testing of orifice plates to be built into the rigid piping system. Since the fluid stroke reaches the meter-range for small fluid-structural mass ratios, the frequency range of application must be limited to keep the fluid-gas interface intact. Mechanical membranes at this interface are undesirable since they would immediately cause a lifetime problem. Reiterer in his dissertation [5], see also [6], extended the application of the TLCGD to mitigate coupled flexural and torsional vibrations of long-span bridges by keeping the simple modal tuning procedure in the analogy to an equivalent TMD. Since vertical and torsional forcing render parametric excitation of the fluid flow, Reiterer and Ziegler [7] presented the cut-off values of the damping to surely avoid any undesirable disturbance of the TLCGD damping effects. Recently, Fu [8], see also Ziegler and Fu [9] generalized the modal-tuning analogy of the TLCGD for applications in moderately plan-asymmetric high-rise buildings (space frames). In a first condensation procedure of the spatial dynamic system, three degrees of freedom (DOF) are assigned to each floor to account for its horizontal in-plane motion. Considering the modal centers of velocity of that in-plane rigid body floor motion decide about the optimal placement of the TLCGD if the translational motion dominates, i.e., if the center of velocity falls outside of the floor plan. On the contrary, the rotational motion of the floor dominates in strongly asymmetric buildings with several low-frequency modal centers of velocity lying inside of the floor plan. In that case, with a recognizable modal participation factor understood, the torsional TTLCGD, redesigned by bending the horizontal pipe section of the U-shaped TLCGD to a nearly closed curve around the modal center of velocity provides an even more efficient liquid absorber when compared to the U- or V-shaped TLCGD with one and the same amount of fluid-mass.

A novel "pipe-in-pipe" design of a so-called VTLCGD was invented by Reiterer and Ziegler [10] to mitigate vertical vibrations of bridges and equally well of wide-span floor plates. Modal tuning by analogy to an equivalent spring-mass-damper (TMD) has been made possible [11].

To explore the limits of the piston theory currently applied to the motion of the fluid-gas-interface, e.g., of the water-air-contact surface, needs a careful analysis by experts in fluid dynamics. Recently, *Wilhelm Schneider* and his research group [12–14] considered such a moving contact line with weak viscosity effects in numerical simulations with experimental verifications. A nondimensional formulation of the Navier–Stokes equations, the continuity equation and the boundary conditions resulted by scaling the relevant variables by means of the capillary length, the stagnation pressure, the hydrostatic pressure difference, the equilibrium value of the surface tension and the surface density (corresponding to zero surface tension). Schneider and his group demonstrate that the dynamic contact angle increases less rapidly with the interface speed in the presence of prewetting of the pipe wall. Most importantly, this prewetting effect applies to the (low frequency) vibrational fluid motion considered in this paper. Hence, interpreting their results for a given stroke, the frequency must be limited to keep the relative maximum fluid speed below about 10 m/s for the sake of keeping the fluid–gas interface intact and to avoid the dynamic contact angle to reach 180°.

Historically, open TLCDs date back to the early 20th century, when the German shipbuilder Frahm invented anti-rolling tanks to minimize the ship's roll induced by wave motion, see, e.g., Den Hartog [15]. Due to their salient features and with applications to civil engineering structures, TLCDs have caused an increased research interest in the last decade, resulting in both analytical and experimental analyses, for earlier papers see, e.g., [16–19]. For analytical and numerical investigations, the TLCD is usually modeled as a single degree of freedom oscillator that is rigidly attached to the vibrating host structure. Teramura and Yoshida [20] have implemented a bidirectional vibration control system based on TLCDs on a 26-story, 106 m high hotel in Japan. TLCD and TTLCD are proposed to mitigate the vibrations of large offshore platforms [21]. Recently, attempts are being made to replace the tuned liquid damper (TLD, relying on fluid sloshing in a rigid tank) by V-shaped TLCD, even in those applications where the TLD was found ideally suited, e.g., for giant, 100 m high offshore wind turbines [22].

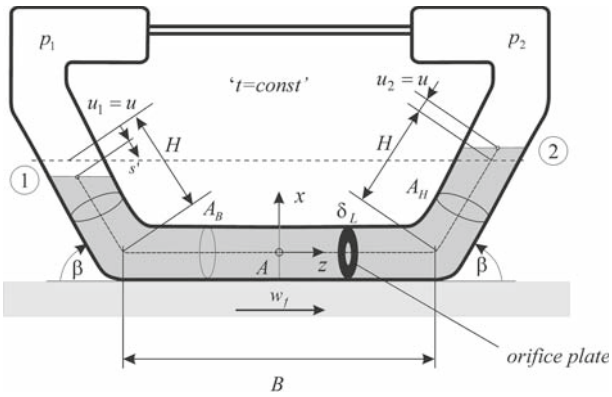

Fig. 1 TLCGD attached to a horizontally, collinear moving frame with an instant "relative" streamline, 1–2, shown, see also [3]

2 General description of a TLCGD when attached to a floor in general horizontal rigid body motion

Several different TLCD geometries have been proposed in the literature, commonly based on the plane symmetrically U-shaped tank. The original design consists of one horizontal and two vertical pipe elements with piecewise constant cross sectional areas. A simple modification renders the more flexible symmetrically V-shaped TLCD where the upright pipe sections are inclined (with opening angle $\pi/4 \leq \beta \leq \pi/2$), as shown in Fig. 1. More complicated geometries, e.g., gradually varying cross sections, curved pipe elements or an asymmetric geometry work similarly, however, often at the price of a nonlinear dynamic system behavior, see, e.g., Gao et al. [16] or, in a general setting, Ziegler [23, p. 495]. To increase the energy dissipation by turbulent damping, an orifice plate can be inserted into the liquid path. To extend the frequency range of applications we make use of the gas spring effect resulting from the sealing of the upright piping sections.

As the TLCGD housing performs a relative motion with respect to an inertial frame, we project Euler's equation of ideal fluid flow on the instant relative streamline and integrate, keeping the time constant, [23, p. 498] and Fig. 1; the viscous and turbulent damping loss will be added subsequently,

$$\int_1^2 \left(\mathbf{a} \cdot \mathbf{e}'_t\right) \mathrm{d}s' = -2g\, u \sin\beta - (p_2 - p_1)/\rho. \tag{1}$$

$\mathbf{a}, \mathbf{e}'_t$, denote the absolute acceleration of the fluid particles along the relative streamline and the tangential direction, respectively. $g, u(t), p, \rho, s'$ are the constant of gravity, the fluid stroke, the absolute pressure, the constant liquid density and the arc-length along the relative streamline, respectively. The indices 1 and 2 refer to the instant positions of the fluid-gas interfaces, Fig. 1. Considering the floor motion generalized with respect to that shown in Fig. 1 by the horizontal in-plane acceleration $\mathbf{a}_A$ of the reference point A and a rotation about the vertical axis with the angular velocity $\dot\theta\, \mathbf{e}_x$, the guiding acceleration of a fluid particle becomes—position of a fluid particle with respect to point A is delineated $\mathbf{r}' = \mathbf{r}'_{y'z'} + x\mathbf{e}_x$

$$\mathbf{a}_g = \mathbf{a}_A + \ddot\theta\, \hat{\mathbf{r}}'_{y'z'} - \dot\theta^2 \mathbf{r}'_{y'z'}, \quad \hat{\mathbf{r}}'_{y'z'} = \mathbf{e}_x \times \mathbf{r}'_{y'z'}. \tag{2}$$

The *Coriolis* acceleration $\mathbf{a}_c = 2\dot\theta\, \dot u\, (s', t)\, (\mathbf{e}_x \times \mathbf{e}'_t)$ is orthogonal to the relative streamline, and the tangential component of the relative acceleration in *Eulerian* decomposition is in general determined by

$$\left(\mathbf{a}' \cdot \mathbf{e}'_t\right) = \frac{\partial' \dot u}{\partial t} + \frac{\partial}{\partial s'}\left(\frac{\dot u^2}{2}\right). \tag{3}$$

Hence, the absolute acceleration $\mathbf{a}$ of a liquid particle when projected on the relative streamline becomes

$$\left(\mathbf{a} \cdot \mathbf{e}'_t\right) = \left(\mathbf{a}_A \cdot \mathbf{e}'_t\right) - \dot\theta^2 \left(\mathbf{r}'_{y'z'} \cdot \mathbf{e}'_t\right) + \frac{\partial' \dot u}{\partial t} + \frac{\partial}{\partial s'}\left(\frac{\dot u^2}{2}\right). \tag{4}$$

Performing partly the integration in Eq. (1) yields (see again Fig. 1 for the integration path)

$$\int_1^2 \frac{\partial' \dot{u}}{\partial t}\,\mathrm{d}s' = -2g\,u\sin\beta - \frac{1}{\rho}\,(p_2 - p_1) - \int_1^2 \left[\left(\mathbf{a}_A \cdot \mathbf{e}'_t\right) - \dot{\theta}^2\left(\mathbf{r}'_{y'z'} \cdot \mathbf{e}'_t\right)\right]\mathrm{d}s', \tag{5}$$

where symmetry in $\int_1^2 \frac{\partial}{\partial s'}(\dot{u}^2/2)\,\mathrm{d}s' = \frac{1}{2}(\dot{u}_2^2 - \dot{u}_1^2) = 0$ has been considered. Apparently, Eq. (5) is extended on the right-hand side by $-\int_1^2 (\mathbf{a}_g \cdot \mathbf{e}'_t)\,\mathrm{d}s'$, accounting for the moving reference frame. The first part of the integration is easily performed when using the unit vector $\mathbf{e}'_A$ in the rotated trace of the TLCGD mid-plane in the floor, coinciding with the tangential vector $\mathbf{e}'_t$ within the horizontal pipe section of length B; in the reference configuration its direction is given by $(\mathbf{e}_A \cdot \mathbf{e}_y) = \cos\gamma$:

$$\int_1^2 \left(\mathbf{a}_A \cdot \mathbf{e}'_t\right)\,\mathrm{d}s' = (B + 2H\cos\beta)\left(\mathbf{a}_A \cdot \mathbf{e}'_A\right). \tag{6}$$

The rotational term apparent in the second term of the integral on the right-hand side of Eq. (5) eventually causes parametric excitation of the relative fluid flow,

$$-\dot{\theta}^2 \int_1^2 \left(\mathbf{r}'_{y'z'} \cdot \mathbf{e}'_t\right)\,\mathrm{d}s' = -\dot{\theta}^2 u\,(B + 2H\cos\beta)\cos\beta. \tag{7}$$

The difference of the internal gas pressures acting at the free liquid surfaces, $p_2 - p_1$, in Eq. (5) vanishes approximately for a free gas stream from point 2 to 1 as allowed in the classical TLCD design with a pipe connection carrying the alternating gas flow. When sealing the gas volume to $V_a = A_H H_a$ on each side of the TLCGD, Fig. 1, a quasi-static approach can be applied to approximate the pressure difference, since the operating range is limited to low frequencies. In the weakly nonlinear polytropic material law for gases, $(p/p_0) = (\rho/\rho_0)^n$, the ratio of the gas densities for a given fluid stroke u is given by $V_a/(V_a \pm A_H u)$, where p_0, $1 \le n \le 1.4$, denote the equilibrium gas pressure and the polytropic index, respectively. A Taylor series expansion of the pressure at its equilibrium value renders for the relevant difference,

$$p_2 - p_1 = 2n\,p_0\,u/H_a + O\,(u/H_a)^3\,. \tag{8}$$

The linear term in Eq. (8) suffices, when limiting the compression ratio to $\max|u|/H_a \le 0.3$, checked in [2]. Under this condition and with the nonstationary integral in Eq. (5) evaluated in the standard form as $\ddot{u}\,L_{\mathrm{eff}}$, the equation of the relative incompressible fluid flow can be expressed in terms of the fluid stroke, with the experimentally observed averaged turbulent damping added: $\Delta p_L/\rho L_{\mathrm{eff}} = \delta_L\,|\dot{u}|\,\dot{u}$, with the head loss coefficient $\delta_L = \lambda/2L_{\mathrm{eff}}$,

$$\begin{aligned} &\ddot{u} + \delta_L\,|\dot{u}|\,\dot{u} + \omega_A^2\left(1 - \kappa\cos\beta\,\dot{\theta}^2/\omega_A^2\right)u = -\kappa\left(\mathbf{a}_A \cdot \mathbf{e}'_A\right), \\ &\kappa = (B + 2H\cos\beta)/L_{\mathrm{eff}}, \quad L_{\mathrm{eff}} = 2H + BA_H/A_B. \end{aligned} \tag{9}$$

The linear frequency in Eq. (9) is expressed in a suitable form for comparison's sake with a mathematical pendulum of length L_0 having the same period,

$$f_A = \frac{\omega_A}{2\pi} = \frac{\sqrt{(g/\pi^2)\,(\sin\beta + h_0/H_a)}}{\sqrt{4\,(L_{\mathrm{eff}}/2)}}, \quad h_0 = np_0/\rho g, \quad \rho_{\mathrm{water}} = 1000\,\mathrm{kg/m^3}, \quad f_A = \frac{\sqrt{(g/\pi^2)}}{\sqrt{4L_0}}. \tag{10}$$

Thus, in the design stage of the TLCGD, the gas equilibrium pressure required to match the optimal frequency can be expressed in terms of the ratio "effective fluid column length to the length of the equivalent mathematical pendulum",

$$h_0/H_a = L_{\mathrm{eff}}/2L_0 - \sin\beta. \tag{11}$$

Careful investigations in [12–14] limit the maximum allowable (relative) speed of the fluid to $|\dot{u}| = \omega_A|u| < 10\,\mathrm{m/s}$ to keep the fluid-gas interface intact. Hence, for a given fluid stroke, the practicable range of the frequency in Eq. (10) is bounded.

In the course of the tuning process the parametric excitation in Eq. (9) is neglected and the nonlinear damping is equivalently linearized. Assuming a time harmonic motion, the work dissipated in one cycle renders the corresponding amplitude dependent linear damping coefficient [2]

$$\zeta_A = (4/3\pi)\ \delta_L \max|u| \tag{12}$$

to be substituted in the equation of motion of the relative fluid flow:

$$\ddot{u} + 2\zeta_A\,\omega_A\,\dot{u} + \omega_A^2\,u = -\kappa\,\left(\mathbf{a}_A\cdot\mathbf{e}'_A\right), \quad \left(\mathbf{a}_A\cdot\mathbf{e}'_A\right) = a_{Ay}\cos(\gamma+\theta) + a_{Az}\sin(\gamma+\theta), \tag{13}$$

where ω_A and κ are the linear natural circular frequency, Eq. (10), and the geometry-dependent excitation influence factor, Eq. (9), respectively. Delineation in the un-primed coordinates in the undisturbed reference system renders the forcing nonlinear; see Eq. (13). With respect to the center of floor mass C_M, the acceleration of point A becomes

$$\mathbf{a}_A = a_{Ay}\,\mathbf{e}_y + a_{Az}\,\mathbf{e}_z = \mathbf{a}_{C_M} + \ddot{\theta}\,\hat{\mathbf{r}}_{AC_M} - \dot{\theta}^2\,\mathbf{r}_{AC_M}, \quad \mathbf{r}_{AC_M} = \left(y_A - y_{C_M}\right)\mathbf{e}_y + \left(z_A - z_{C_M}\right)\mathbf{e}_z. \tag{14}$$

To make use of the substructure synthesis of the TLCGD to the floor we need to determine the resultants of the fluid motion by means of the conservation laws of momentum and moment of momentum. The dead weight of the piping system is added to the floor mass. The position of the fluid's center of mass C_f is $\mathbf{r}_f = \mathbf{r}_A + s'_f\mathbf{e}'_A + x_f\mathbf{e}_x$, where the static fluid mass moments render $s'_f = \bar{\kappa}u$ and $x_f = \bar{\kappa}_1\left(H^2+u^2\right)/2H$, and hence,

$$\bar{\kappa} = \kappa L_{\text{eff}}/L_1, \quad \kappa_1 = (2H/L_{\text{eff}})\sin\beta, \quad \bar{\kappa}_1 = \kappa_1 L_{\text{eff}}/L_1, \quad m_f = \rho A_H L_1, \quad L_1 = 2H + BA_B/A_H. \tag{15}$$

The acceleration of C_f,

$$\mathbf{a}_f = \frac{d^2\mathbf{r}_f}{dt^2} = \mathbf{a}_A + \bar{\kappa}\left(\ddot{u} - u\,\dot{\theta}^2\right)\mathbf{e}'_A + \bar{\kappa}\left(u\,\ddot{\theta} + 2\dot{u}\,\dot{\theta}\right)\hat{\mathbf{e}}'_A + \frac{\bar{\kappa}_1}{H}\left(\dot{u}^2 + u\,\ddot{u}\right)\mathbf{e}_x, \tag{16}$$

determines the resulting force and, as well the control force acting along the trace; note that, a roof denotes the positively rotated orthogonal in-plane vector,

$$\mathbf{F}_A = m_f\mathbf{a}_f, \quad \mathbf{F}_c = \bar{\kappa}m_f\left(\ddot{u} - u\,\dot{\theta}^2\right)\mathbf{e}'_A \tag{17}$$

The in-plane force components in the un-primed reference coordinates are listed below; see also Eq. (14),

$$\begin{aligned} F_{Ay} &= m_f\left[a_y + \bar{\kappa}\left(\ddot{u} - u\,\dot{\theta}^2\right)\cos(\gamma+\theta) - \bar{\kappa}\left(u\,\ddot{\theta} + 2\dot{u}\,\dot{\theta}\right)\sin(\gamma+\theta)\right], \\ F_{Az} &= m_f\left[a_z + \bar{\kappa}\left(\ddot{u} - u\,\dot{\theta}^2\right)\sin(\gamma+\theta) + \bar{\kappa}\left(u\,\ddot{\theta} + 2\dot{u}\,\dot{\theta}\right)\cos(\gamma+\theta)\right]. \end{aligned} \tag{18}$$

The axial moment about the vertical axis, with respect to the reference point A, is explicitly evaluated by conservation of the angular momentum; the other two axial moments about the axes in the orthogonal directions $\mathbf{e}'_A$ and $\hat{\mathbf{e}}'_A$ are undesirable and are not further discussed here,

$$\begin{aligned} M_{Ax} &= m_f\left[\bar{\kappa}_3 H^2\,\ddot{\theta} + \bar{\kappa}\left(u^2\,\ddot{\theta} + 2u\,\dot{u}\,\dot{\theta}\right)\cos\beta + \bar{\kappa}u\left(\hat{\mathbf{e}}'_A\cdot\mathbf{a}_A\right)\right], \\ \bar{\kappa}_3 &= \tfrac{B}{L_1}\left[\left(\tfrac{B}{2H}\right) + \tfrac{A_B}{3A_H}\left(\tfrac{B}{2H}\right)^2 + \left(1 + \tfrac{2H}{3B}\cos\beta\right)\cos\beta\right]. \end{aligned} \tag{19}$$

Linearization of Eq. (19) together with the assumption $|\theta| \ll 1$ saves the first term of the moment in Eq. (19).

3 A moderately asymmetric single storey space frame with a TLCGD attached

Three degrees of freedom are assigned to the rigid floor with displacements v and w of the floor's center of mass C_M and (small) rotation θ about the vertical axis determining the deformation. A single point horizontal base excitation, seismogram $a_g(t)$, with arbitrary angle of attack α against the y-axis, $\ddot{v}_g = a_g(t)\cos\alpha$, $\ddot{w}_g = a_g(t)\sin\alpha$, refers to a simple model of seismic action; soil-structure interaction is neglected. The supporting columns may have anisotropic flexural stiffness and the center of stiffness may be disjoint from the center of mass. Commonly the geometric correction of the flexural stiffness is applicable to account for the compressive normal force produced by the floor's dead weight, see, e.g., [23, p. 604], however note in this case the *Hermite* shape function H_3 on p. 611 for the more standard approximation of the (static) deflection of a clamped–clamped beam. In some cases, modal portions of the column mass must be added to the floor with one and the same shape function taken into account. With mass- and stiffness matrices known, a modal analysis is performed rendering the natural (circular) frequencies ω_j and mode shapes $\vec{\phi}_j$, $j = 1, 2, 3$. Next, the modal centers of velocity are determined to decide about the strength of the asymmetry: Ziegler [23, p. 14] provides the formulas for this point in the floor with instantly vanishing velocity. For small deformations, time can be eliminated and the displacements are determined by a small rotation about the center: to preserve the dimension length, the angle of rotation is commonly multiplied by the radius of inertia of the floor, $u_T = r_S\,\theta$, $(v\ w\ u_T)_j = q_j(t)\phi_{jk}$, $k = 1, 2, 3$,

$$\mathbf{r}_{C_{vj}C_M} = \begin{Bmatrix} y_{C_{vj}} - y_{C_M} \\ z_{C_{vj}} - z_{C_M} \end{Bmatrix} = r_S \begin{Bmatrix} -\phi_{j\,2}/\phi_{j\,3} \\ \phi_{j\,1}/\phi_{j\,3} \end{Bmatrix}. \tag{20}$$

Thus, the modal displacements of a point P in the floor are approximately given by, $|\theta| \ll 1$,

$$\begin{Bmatrix} v_P \\ w_P \end{Bmatrix} = \left(\phi_{j\,3}/r_S\right)\hat{\mathbf{r}}_{P\,C_{vj}}, \quad \hat{\mathbf{r}}_{P\,C_{vj}} = \begin{Bmatrix} -\left(z_P - z_{C_{vj}}\right) \\ y_P - y_{C_{vj}} \end{Bmatrix}. \tag{21}$$

Figure 2 illustrates the case of moderate asymmetry where all modal centers of velocity are lying outside of the floor plan, indicating dominating displacements for small rotation, and it shows the proper arrangement of three modally tuned TLCGDs on the floor with their normal distance to the corresponding modal center of velocity "maximum".

Modal expansion of the main structural equations of motion with the coupling forces to the TLCGD substituted, however in their linearized form, Eqs. (18) and (19), with a single point oblique base excitation considered, namely

$$F_{Ay} = m_f\left[\ddot{v}_g + \ddot{v} - \left(z_A - z_{C_M}\right)\ddot{\theta}\ \right] + \bar{\kappa} m_f \ddot{u}\cos\gamma, \quad F_{Az} = m_f\left[\ddot{w}_g + \ddot{w} + \left(y_A - y_{C_M}\right)\ddot{\theta}\right] + \bar{\kappa} m_f \ddot{u}\sin\gamma \tag{22}$$

render, upon projection on the mode numbered j,

$$\begin{bmatrix} 1+\mu_j & \bar{\kappa}\left(v_{Aj}\cos\gamma + w_{Aj}\sin\gamma\right) m_{fj}/m_j \\ \kappa\left(v_{Aj}\cos\gamma + w_{Aj}\sin\gamma\right) & 1 \end{bmatrix} \begin{bmatrix} \ddot{q}_j \\ \ddot{u} \end{bmatrix} + \begin{bmatrix} 2\zeta_{Sj}\omega_{Sj} & 0 \\ 0 & 2\zeta_{Aj}\omega_{Aj} \end{bmatrix} \begin{bmatrix} \dot{q}_j \\ \dot{u} \end{bmatrix}$$
$$+ \begin{bmatrix} \omega_{Sj}^2 & 0 \\ 0 & \omega_{Aj}^2 \end{bmatrix} \begin{bmatrix} q_j \\ u \end{bmatrix} = -\begin{bmatrix} \vec{L}_j^T/m_j \\ \kappa \mathbf{r}_S^T \end{bmatrix} \ddot{\mathbf{x}}_g. \tag{23}$$

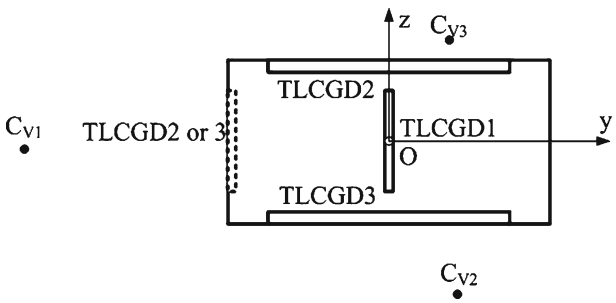

Fig. 2 Modal centers of velocity • of a moderately asymmetric space frame (length scale applies), [9]. Positioning of three TLCGDs (modally tuned) with an alternative shown

The generalized participation factors become, with the total floor mass M_S,

$$\mathbf{L}_j^T = \begin{bmatrix} L_{jy} & L_{jz} & 0 \end{bmatrix}, \quad L_{jy} = M_S\phi_{j1} + m_{fj}v_{Aj}, \quad L_{jz} = M_S\phi_{j2} + m_{fj}w_{Aj}. \tag{24}$$

The properly generalized modal fluid mass ratio with $m_j = \vec{\phi}_j^T \mathbf{M}_S \vec{\phi}_j$, the modal mass of the main system and m_{fj} the fluid mass in the TLCGD numbered j, depends on the location of the reference point $A\ (y_A\ z_A\ 0)$, and should be maximum,

$$\mu_j = \frac{m_{fj}}{m_j} V_j^2 \to \max|_A, \quad V_j^2 = V_j^{*2} + \bar{\kappa}_3 \left(\phi_{j3} H / r_S\right)^2, \quad V_j^{*2} = v_{Aj}^2 + w_{Aj}^2. \tag{25}$$

The TLCGD Eq. (13) when further linearized with respect to the forcing, and with the modal values substituted, is given by

$$\begin{aligned} &\ddot{u} + 2\zeta_{Aj}\omega_{Aj}\dot{u} + \omega_{Aj}^2 u = -\kappa \left[\left(v_{Aj}\cos\gamma + w_{Aj}\sin\gamma\right) \ddot{q}_j + \left(\mathbf{r}_S^T \cdot \ddot{\mathbf{x}}_g\right) \right], \quad \mathbf{r}_S^T = \begin{bmatrix} \cos\gamma & \sin\gamma & 0 \end{bmatrix}, \\ &\ddot{\mathbf{x}}_g^T = \begin{bmatrix} \ddot{v}_g & \ddot{w}_g & 0 \end{bmatrix}, \quad v_{Aj} = \phi_{j1} - \phi_{j3}\left(z_{Aj} - z_{C_M}\right)/r_S, \quad w_{Aj} = \phi_{j2} + \phi_{j3}\left(y_{Aj} - y_{C_M}\right)/r_S \end{aligned} \tag{26}$$

and has been inserted into Eq. (23) to approximately make modal decoupling possible, well separated natural frequencies of the main structure are thus understood.

Following the tuning procedure by analogy, originally developed by Hochrainer [2], we put an equivalent TMD of the spring-mass-dashpot type at reference point A, with relative displacement u^* in the direction γ, on the floor. Since the parameters of the main system, namely mass, natural frequency, and light modal damping are subjected to change in this case, they are marked by asterisks; a modal expansion renders

$$\begin{aligned} &\begin{bmatrix} 1+\mu_j^* & \left(v_{Aj}\cos\gamma + w_{Aj}\sin\gamma\right) m_{Aj}^*/m_j^* \\ \left(v_{Aj}\cos\gamma + w_{Aj}\sin\gamma\right) & 1 \end{bmatrix} \begin{bmatrix} \ddot{q}_j \\ \ddot{u}^* \end{bmatrix} + \begin{bmatrix} 2\zeta_{Sj}^*\omega_{Sj}^* & 0 \\ 0 & 2\zeta_{Aj}^*\omega_{Aj}^* \end{bmatrix} \begin{bmatrix} \dot{q}_j \\ \dot{u}^* \end{bmatrix} \\ &+ \begin{bmatrix} \omega_{Sj}^{*2} & 0 \\ 0 & \omega_{Aj}^{*2} \end{bmatrix} \begin{bmatrix} q_j \\ u^* \end{bmatrix} = - \begin{bmatrix} \mathbf{L}_j^{*T}/m_j^* \\ \mathbf{r}_S^T \end{bmatrix} \ddot{\mathbf{x}}_g, \\ &L_{jy}^* = M_S^*\phi_{j1} + m_{Aj}^* v_{Aj}, \quad L_{jz}^* = M_S^*\phi_{j2} + m_{Aj}^* w_{Aj}, \end{aligned} \tag{27}$$

where M_S^* is the floor mass of the equivalent main system, and the TMD equation of motion has been inserted,

$$\ddot{u}^* + 2\zeta_{Aj}^*\omega_{Aj}^*\dot{u}^* + \omega_{Aj}^{*2}u^* = -\left(v_{Aj}\cos\gamma + w_{Aj}\sin\gamma\right)\ddot{q}_j - \left(\mathbf{r}_S^T \cdot \ddot{\mathbf{x}}_g\right). \tag{28}$$

Requiring the forcing in Eqs. (26) and (28) to be equal, yields at once the proportionality

$$u = \kappa u^* \tag{29}$$

and, upon substitution in the second of Eqs. (23) and (27), leaves the natural frequency and the linear damping of both absorbers unchanged. Substituting these results in the first of the Eqs. (23) and (27) defines the transformations of the main system parameters and the modal absorber mass ratio. By some algebraic manipulations the mass ratio of the equivalent TMD results,

$$\mu_j^* = \mu_j \frac{\kappa\bar{\kappa}\left(V_j^*/V_j\right)^2}{1 + \mu_j\left[1 - \kappa\bar{\kappa}\left(V_j^*/V_j\right)^2\right]} < \mu_j \tag{30}$$

together with the transformation of the optimal frequency ratio, linear damping remaining unchanged,

$$\delta_{j\mathrm{opt}} = \frac{f_{Aj\mathrm{opt}}}{f_{Sj}} = \frac{\delta_{j\mathrm{opt}}^*}{\sqrt{1 + \mu_j\left[1 - \kappa\bar{\kappa}\left(V_j^*/V_j\right)^2\right]}} < \delta_{j\mathrm{opt}}^*, \quad \zeta_{Aj\mathrm{opt}} = \zeta_{Aj\mathrm{opt}}^*. \tag{31}$$

Thus, having determined the TLCGD geometry, the analogue TMD modal system can be used to obtain the optimal tuning frequency and the best damping ratio from literature, e.g., [15], [24] and [25] and to apply these

parameters to optimize the TLCGD design, Eqs. (10) and (11). To render the absolute acceleration of point A in direction $\mathbf{e}_A$ minimum, the Den Hartog formula gives very good results even if small modal structural damping is considered, μ_j^* of Eq. (30) substituted,

$$\delta_{j\text{opt}}^* = f_{Aj\text{opt}}^* \Big/ f_{Sj}^* = 1/\left(1+\mu_j^*\right), \quad \zeta_{Aj\text{opt}}^* = \sqrt{3\mu^*/8\left(1+\mu_j^*\right)}. \tag{32}$$

If several TLCGDs are applied, subsequent fine-tuning, e.g., by minimizing a performance index in the frequency state space, is recommended, see [4,6]. The Den Hartog optimal parameters serve as the initial values, e.g., in the standard program *fminsearch* of MATLAB [26].

A numerical simulation of the space frame with three TLCGDs attached and with modes according to Fig. 2 was performed, [9], varying the angle of attack $0 \leq \alpha < \pi$ of the ground acceleration "1940 El Centro seismogram" scaled to 0.35 g maximum acceleration. At the critical angle $\alpha \simeq \pi/6$, all three TLCGDs were active to effectively reduce the severe response of the main system. However, the maximum fluid strokes and thus, the maximum relative fluid speeds occurred at $\alpha \simeq \pi/2$ with 3.0 m/s in TLCGD1, at $\alpha \simeq 0$ in TLCGDs 2 and 3 with 3.2 and 2.9 m/s, respectively, all are well within the limit given in [12]. Thus the fluid-gas interface remains intact.

4 A strongly asymmetric space frame with TTLCGD attached

Again, such a single storey space frame is considered exemplarily, to illustrate the action of a TTLCGD in the ith floor of an N-storey tall building with a straightforward generalization understood. The modal analysis is performed likewise to the previous section; however, if several modal centers of velocity fall into the floor plan, Fig. 3, strong asymmetry is "defined".

According to the example illustrated in Fig. 3, torsion dominates the coupled vibrations of the first two modes. Consequently, (torsional) TTLCGDs are applied and modally tuned. To derive their equations of motion, in Eq. (5) the integration path has to be changed since the horizontal pipe section of length B is now a nearly closed loop and, in this case, the upright pipe sections are assumed to be vertical, $\beta = \pi/2$, and set at a reference point $A\left(y_A\ z_A\ 0\right)$ to be properly selected in the course of maximizing the modal mass ratio. Commonly, the TTLCGDs have a doubly symmetric horizontal pipe section with respect to C_M. Hence, we choose the geometric center O that coincides with the center of mass C_M of the floor for the uniformly distributed floor-mass to delineate the guiding acceleration in Eq. (2) with respect to $C_M = O$:

$$\mathbf{a}_g = \mathbf{a}_{C_M} + \ddot{\theta}\hat{\mathbf{r}}'_{y'z'} - \dot{\theta}^2\mathbf{r}'_{y'z'}. \tag{33}$$

The integral on the right-hand side of Eq. (5) when considering the curved doubly symmetric horizontal path of integration and putting $\beta = \pi/2$, reduces to

$$\int_1^2 \mathbf{a}_g \cdot \mathbf{e}'_t \, \mathrm{d}s' = \ddot{\theta} \oint_B \hat{\mathbf{r}}'_{y'z'} \cdot \mathbf{e}'_t \, \mathrm{d}s' = 2A_p\,\ddot{\theta}, \tag{34}$$

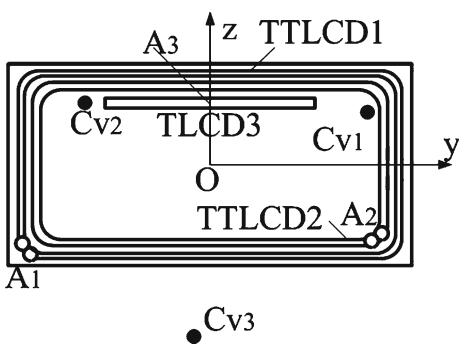

Fig. 3 Modal centers of velocity • of a strongly asymmetric space frame (length scale applies), [9]: those of the first two modes fall inside the floor plan. Proper positioning of two TTLCGDs and one TLCGD (modally tuned)

where A_p is the area enclosed by the looping axis of the horizontal pipe section. The angle of rotation about the vertical axis θ is changed to the newly defined variable of dimension length by multiplication with the radius of inertia of the fluid mass with respect to point $O = C_M$: $u_{TT} = r_f\theta$. Finally, the linear damping equivalent to the averaged turbulent damping is considered in the linearized TTLCGD equation of relative fluid motion,

$$\ddot{u} + 2\zeta_A\omega_A\dot{u} + \omega_A^2 u = -\kappa_{T0}\ddot{u}_{TT}, \quad \kappa_{T0} = \frac{2A_P}{r_f L_{\text{eff}}},$$
$$I_{fx}\big|_{O=C_M} = m_f r_f^2 = \rho A_H \left[\frac{A_B}{A_H}\oint_B \mathbf{r}'^2_{y'z'}\,\mathrm{d}s' + 2H\left(y_A^2 + z_A^2\right)\right], \tag{35}$$

with linear frequency still defined by Eq. (10), see Hochrainer [2] for the first considerations without any discussion of the tuning procedure.

The resultants of the fluid motion in the TTLCGD, referred to $O = C_M$, are given by substituting the acceleration of the fluid's center of mass into the first Eq. (17),

$$\mathbf{a}_f = \mathbf{a}_{C_M} + \frac{2H}{L_1}\left[-\left(z_A\ddot{\theta} + y_A\dot{\theta}^2\right)\mathbf{e}_{y'} + \left(y_A\ddot{\theta} - z_A\dot{\theta}^2\right)\mathbf{e}_{z'} + \frac{1}{H}\left(\dot{u}^2 + u\ddot{u}\right)\mathbf{e}_x\right]. \tag{36}$$

The linearized components of the interaction force in the unprimed reference coordinates become

$$F_y\big|_{O=C_M} = m_f\left(\ddot{v}_g + \ddot{v} - 2H\,\ddot{u}_{TT}z_A/L_1\,r_f\right), \quad F_z|_{O=C_M} = m_f\left(\ddot{w}_g + \ddot{w} + 2H\,\ddot{u}_{TT}y_A/L_1\,r_f\right). \tag{37}$$

Equation (19) changes to

$$M_x|_{O=C_M} = m_f r_f^2\left[\ddot{\theta} + \left(2H/L_1 r_f^2\right)\left(y_A a_z - z_A a_y\right)_{C_M} + \bar{\kappa}_{T0}\ddot{u}/r_f\right], \quad \bar{\kappa}_{T0} = \kappa_{T0}L_{\text{eff}}/L_1. \tag{38}$$

With modal values numbered j substituted in Eq. (35) and with linearized interaction forces considered in the modal equation of the main structure, the alternative to Eqs. (23) and (25) reads,

$$\begin{bmatrix} 1+\mu_j & \bar{\kappa}_{T0}\phi_{j3}m_{fj}r_{fj}/m_j r_S \\ \kappa_{T0}\phi_{j3}r_{fj}/r_S & 1 \end{bmatrix}\begin{bmatrix}\ddot{q}_j \\ \ddot{u}\end{bmatrix} + \begin{bmatrix} 2\zeta_{Sj}\omega_{Sj} & 0 \\ 0 & 2\zeta_{Aj}\omega_{Aj}\end{bmatrix}\begin{bmatrix}\dot{q}_j \\ \dot{u}\end{bmatrix}$$
$$+\begin{bmatrix}\omega_{Sj}^2 & 0 \\ 0 & \omega_{Aj}^2\end{bmatrix}\begin{bmatrix}q_j \\ u\end{bmatrix} = -\begin{bmatrix}\mathbf{L}_{Tj}^T/m_j \\ \mathbf{0}^T\end{bmatrix}\ddot{\mathbf{x}}_g, \tag{39}$$

$$\mu_j = \frac{m_{fj}}{m_j}V_{Tj}^2, \quad V_{Tj}^2 = v_{Tj}^2 + 4H\phi_{j3}\left(y_{Aj}\phi_{j2} - z_{Aj}\phi_{j1}\right)/L_1 r_S \to \max|_{A_j(y_{Aj}\ z_{Aj}\ 0)},$$
$$v_{Tj}^2 = \phi_{j1}^2 + \phi_{j2}^2 + \left(\phi_{j3}r_{fj}/r_S\right)^2. \tag{40}$$

The participation factors are formally still given by Eq. (24); however, before their substitution, the modal displacements of Eq. (26) have to be altered by the substitutions

$$v_{Aj} \to \phi_{j1} - 2H\phi_{j3}z_{Aj}/L_1, r_S, \quad w_{Aj} \to \phi_{j2} + 2H\phi_{j3}y_{Aj}/L_1\,r_S. \tag{41}$$

To perform tuning by analogy to an equivalent (torsional) TTMD, the latter is designed as a torsional spring-mass-dashpot system that moves in translational modal motion with the floor but allows for a relative modal rotation with angular coordinate u^*/r_A^*. The absorber mass is assumed doubly symmetric distributed with respect to the point $C_M = O$, Fig. 4, with the moment of inertia $I_{C_Mx} = m_{Aj}^* r_{Aj}^{*2}$.

The approximating modal system of equations simply becomes, an asterisk denoting all relevant parameters,

$$\begin{bmatrix} 1+\mu_j^* & \phi_{j3}m_{Aj}^* r_{Aj}^*/m_j^* r_S \\ \phi_{j3}r_{Aj}^*/r_S & 1 \end{bmatrix}\begin{bmatrix}\ddot{q}_j \\ \ddot{u}^*\end{bmatrix} + \begin{bmatrix} 2\zeta_{Sj}^*\omega_{Sj}^* & 0 \\ 0 & 2\zeta_{Aj}^*\omega_{Aj}^*\end{bmatrix}\begin{bmatrix}\dot{q}_j \\ \dot{u}^*\end{bmatrix}$$
$$+\begin{bmatrix}\omega_{Sj}^{*2} & 0 \\ 0 & \omega_{Aj}^{*2}\end{bmatrix}\begin{bmatrix}q_j \\ u^*\end{bmatrix} = -\begin{bmatrix}\mathbf{L}_{Tj}^{*T}/m_j^* \\ \mathbf{0}^T\end{bmatrix}\ddot{\mathbf{x}}_g, \tag{42}$$

$$\mu_j^* = \frac{m_{Aj}^*}{m_j^*}v_{Tj}^{*2}, \quad v_{Tj}^{*2} = \phi_{j1}^2 + \phi_{j2}^2 + \left(\phi_{j3}r_{Aj}^*/r_S\right)^2, L_{Tjy}^* = \left(m_S^* + m_{Aj}^*\right)\phi_{j1}, L_{Tjz}^* = \left(m_S^* + m_{Aj}^*\right)\phi_{j2} \tag{43}$$

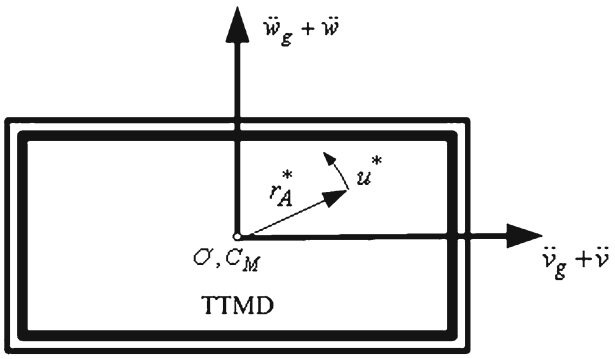

Fig. 4 Floor of the single–storey strongly asymmetric structure with equivalent TTMD: mass with rotational spring support and dashpot, relative angle of rotation u^*/r_A^*

with the selected modal motion of the TTMD considered

$$\ddot{u}^* + 2\zeta_{Aj}^*\omega_{Aj}^*\dot{u}^* + \omega_{Aj}^{*2}u^* = -\ddot{q}_j\phi_{j3}r_{Aj}^*/r_S. \tag{44}$$

The analogy requires one and the same excitation in Eqs. (35) and (44), thus

$$\ddot{u}_{TT} = r_f\ddot{\theta} = \ddot{u}_{TT}^* = r_A^*\ddot{\theta} \rightarrow r_{fj} = r_{Aj}^* \tag{45}$$

rendering at once the proportionality, cf. Eq. (29),

$$u = \kappa_{T0}u^* \tag{46}$$

and, upon substitution in the second (homogeneous) Eqs. (39) and (42), leaves the natural frequency and the linear damping coefficient of both absorbers unchanged (analogous to the TLCGD). Inspection of the first of Eqs. (39) and (42) defines the transformation of the main system parameters and, most importantly, the modal absorber mass ratio, cf. Eq. (30) of the TLCGD,

$$\mu_j^* = \mu_j \frac{\kappa_{T0}\bar{\kappa}_{T0}\left(v_{Tj}/V_{Tj}\right)^2}{1 + \mu_j\left[1 - \kappa_{T0}\bar{\kappa}_{T0}\left(v_{Tj}/V_{Tj}\right)^2\right]} < \mu_j, \quad v_{Tj}^* = v_{Tj}. \tag{47}$$

The transformation of the optimal frequency ratio becomes, cf. Eq. (31), valid for TLCGD, optimal linear damping remains unchanged for TTMD and TTLCGD, the Den Hartog optimal parameters of Eq. (32) can be selected and substituted,

$$\delta_{j\text{opt}} = \frac{f_{Aj\text{opt}}}{f_{Sj}} = \frac{\delta_{j\text{opt}}^*}{\sqrt{1 + \mu_j\left[1 - \kappa_{T0}\bar{\kappa}_{T0}\left(v_{Tj}/V_{Tj}\right)^2\right]}} < \delta_{j\text{opt}}^*. \tag{48}$$

Remark Outwardly inclined upright sections of the TTLCGD, $\pi/4 \leq \beta < \pi/2$, somewhat increase the active fluid mass and in addition provide a control force at the reference point A with the effect of increasing the control moment of the dominating rotational vibration with respect to $C_M = O$. However, the analogy to an equivalent TTMD becomes more complex: a point mass must be added to the TTMD resulting in quite complex relations, see Fu [8] for details.

4.1 Effective modal damping of the dominating rotational first mode by the TTLCGD

The strongly asymmetric (rather small) single storey space frame with floor mass $m_S = 16 \times 10^3$kg has a basic mode assigned with dominating rotation: with $f_{S1} = 1,40$Hz and $\vec{\phi}_1^T = 10^{-2}\left(0.1868\ -0.5981\ 0.4821\right)$, the radius of inertia of the floor is $r_S = 2.58$ m, Fig. 5. The eccentricity of the center of stiffness C_S may be related to a quite stiff staircase and/or elevator tube, separated from the structural columns.

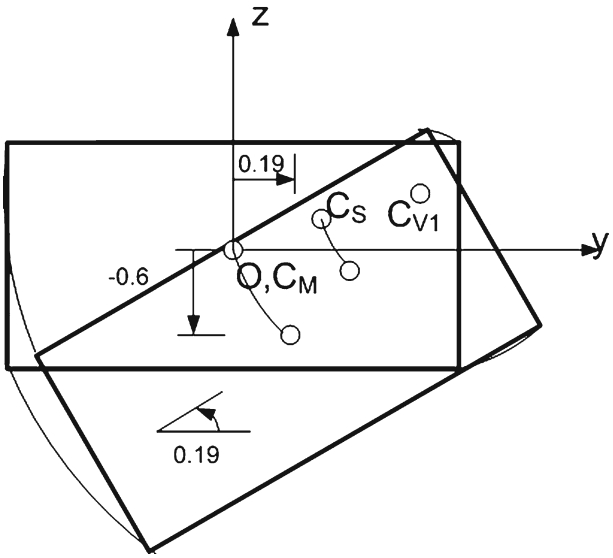

Fig. 5 Fundamental mode with center of velocity C_{v1} shown, rotation exaggerated. Eccentric location of the center of stiffness C_S [8]

Table 1 Layout of the modally tuned TTLCD1, gas volume and gas equilibrium pressure properly assigned [8]

	TTLCD1
Horizontal length of the liquid column B (m)	24
Vertical length of the liquid column H (m)	1.40
Constant cross-sectional area of the pipe (m^2)	0.0187
Effective length $L_{\text{eff}} = L_1 = 2H + B$ (m)	26.80
Angle of the inclined pipe section β (rad)	$\pi/2$
Geometry factor $\kappa_{T0} = \bar{\kappa}_{T0}$	0.67
Equilibrium pressure h_0 (m), Eqs. (10) and (11)	220
Gas volume $V_a = A_H H_a$ (m^3), Eq. (11)	0.0410
Mass ratios μ, μ^*	4.74, 1.81%
Natural frequency $f_{A1\text{opt}}$ (Hz), Eqs. (10) and (48)	1.36
Optimal linear damping $\zeta_{A1\text{opt}}$%, Eq. (32)	8.17

The fluid mass of the TTLCGD 1 is assumed $m_{f1} = 500$kg. It is subjected to tuning to increase the damping of the first mode. The design parameters and the results of Den Hartog tuning by analogy to the equivalent TTMD are listed in Table 1. The rectangular horizontal loop follows closely the border of the floor. Note the rather high equilibrium gas pressure necessary to render the required optimal frequency. The long horizontal loop length B is common in the design of such TTLCGD. The effective modal structural damping coefficient increases from 1% to $\zeta_{eff1} = 6.2$ %, Fig. 6.

5 Tuned liquid column-gas dampers applied to bridges

In case of dominating horizontal or rotational vibrations, the U- or V-shaped TLCGD is well suited to increase effectively the damping of the selected mode. The rigid, symmetrically designed piping system of the absorber is fastened to a properly selected cross-section of the bridge to form a rigid frame with three degrees-of-freedom of the in-plane motion. Note the axis x of rotation of the cross-section is now horizontal; with angle of rotation $|\vartheta| \ll 1$, and y, z are the principal axes of the cross-section when referring to oblique bending. The equation of relative fluid-motion is derived in the form of a generalized Bernoulli equation by integrating along the

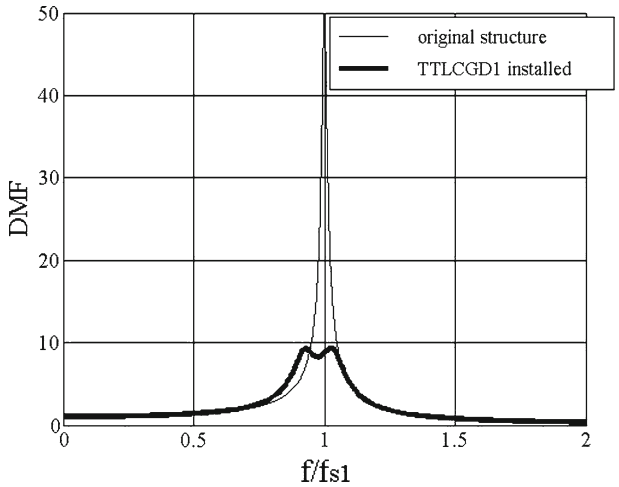

Fig. 6 Dynamic magnification of the first mode in the critical frequency window, without - $\zeta_{S1} = 1\%$ and with linearized TTLCD1 attached, $\zeta_{\text{eff}1} = 6.2\%$. Den Hartog's optimal parameters applied, Eqs. (32), (47), Table 1, [9]

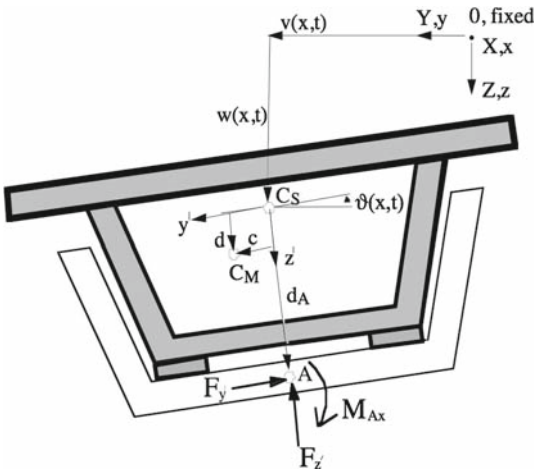

Fig. 7 Single cross section at $x = \xi$ of the bridge (three DOF in-plane motion). Absorber forces applied. Eccentric center of mass C_M. Symmetry in stiffness, center C_S. Note the vertical distance d_A of reference point A with respect to C_S

relative streamline, [23, p. 498], and equivalent linear damping is added, see [6] for details of derivation,

$$\ddot{u} + 2\zeta_A \omega_A \dot{u} + \omega_A^2 \left[1 - \kappa_1 \frac{\ddot{w}}{H\,\omega_A^2} + \left(\kappa_1 \frac{\mathrm{d}_A}{H} - \kappa_2 \right) \frac{\dot{\vartheta}^2}{\omega_A^2}, \right] u = \kappa\,(\ddot{v} - g\vartheta) - \left(\kappa\,\mathrm{d}_A + \kappa_1 \frac{B}{2} \right) \ddot{\vartheta}. \quad (49)$$

Two newly defined geometry coefficients enter Eq. (49); see Eq. (9) for the common coefficient κ,

$$\kappa_1 = (2H/L_{\text{eff}}) \sin\beta, \quad \kappa_2 = (B\cos\beta + 2H)/L_{\text{eff}}. \quad (50)$$

The distance d_A is indicated in Fig. 7. The linear natural frequency is still defined by Eq. (10).

Considering both conservation of momentum and moment of momentum of the fluid body, easily renders the control force components in the rotated coordinates and the moment with respect to point A,

$$F_{y'} = m_f \left\{ a_{y'} - \bar{\kappa} \left(\ddot{u} - u\dot{\vartheta}^2 \right) + \frac{\bar{\kappa}_2}{2H} \left[\left(H^2 + u^2 \right) \ddot{\vartheta} + 4u\dot{u}\dot{\vartheta} \right] \right\},$$
$$F_{z'} = m_f \left\{ a_{z'} - \bar{\kappa} \left(u\ddot{\vartheta} + 2\dot{u}\dot{\vartheta} \right) + \frac{\bar{\kappa}_2}{2H} \left[\left(H^2 + u^2 \right) \dot{\vartheta}^2 - 2 \left(\dot{u}^2 + u\ddot{u} \right) \right] \right\}, \quad (51)$$

$$M_{Ax} = m_f \left[\bar{\kappa}_3' H^2 \ddot{\vartheta} + \frac{\bar{\kappa}_1 B}{2} \ddot{u} - \bar{\kappa} u a_{z'} + \frac{\bar{\kappa}_1}{2H} \left(H^2 + u^2 \right) a_{y'} + \bar{\kappa}_2 \left(u^2 \ddot{\vartheta} + 2 u \dot{u} \dot{\vartheta} \right) \right],$$

$$\bar{\kappa}_1 = \kappa_1 L_{\text{eff}} / L_1, \bar{\kappa}_2 = \kappa_2 L_{\text{eff}} / L_1, \quad \bar{\kappa}_3' = \frac{2H}{3L_1} \left(1 + 3 (B/2H)^2 + \frac{A_B}{A_H} (B/2H)^3 + 3 (B/2H) \cos \beta \right), \quad (52)$$

cf. Eq. (19). If the damping coefficient exceeds the cut-off value of parametric resonance by vertical and rotational motions of the cross-section, parametric excitation in Eq. (49) can be safely neglected.

Extending the more or less coupled partial differential equations of forced, principal flexural and torsional vibrations of a continuous slender beam (rigid in shear, Nowacki [27]) to oblique bending, yield a modal equation within the Galerkin approximation, a single-term Ritz approximation is substituted, Eq. (53), see [23, p. 595]; ($m = \rho A$ is the mass per unit length of the bridge and light modal structural damping has been added, see Fig. 7),

$$v(x,t) = Y(t) \chi(x), \quad w(x,t) = Y(t) \phi(x), \quad u_T(x,t) = e \vartheta(x,t) = Y(t) \psi(x), \quad (53)$$

$$\int_0^l m \left[\chi_i \chi_j + \phi_i \phi_j + \psi_i \psi_j + \frac{c}{e} \left(\psi_i \phi_j + \phi_i \psi_j \right) - \frac{\mathrm{d}}{e} \left(\psi_i \chi_j + \chi_i \psi_j \right) \right] \mathrm{d}x = \begin{bmatrix} 0 & \text{for } i \neq j \\ I_e / e^2 & \text{for } i = j \end{bmatrix}, \quad (54)$$

$$\ddot{Y} + 2 \zeta \Omega \dot{Y} + \Omega^2 Y = \left[-\frac{F_{y'}}{M} \left(\chi + \phi \psi \frac{Y}{e} - \frac{\mathrm{d}_A}{e} \psi \right) - \frac{F_{z'}}{M} \left(\phi - \chi \psi \frac{Y}{e} \right) - \psi \frac{M_{Ax}}{eM} \right]_{x=\xi} + \frac{F(t)}{M}, \quad (55)$$

$$F(t) = \int_0^l \left[\chi(x) \; p_y(x,t) + \phi(x) \; p_z(x,t) + \psi(x) \; \frac{m_x(x,t)}{e} \right] \mathrm{d}x, \quad M = I_e / e^2. \quad (56)$$

Preparation of the (linear) tuning procedure requires the linearized form of the equations of motion of the projected main system with the absorber synthesized. Neglecting parametric forcing in Eq. (49) and substituting the linear dynamic parts of Eq. (51) yields the linearized matrix equation of the coupled modal SDOF-main system with the action of a single TLCGD at a proper position $x = \xi$ considered,

$$\mathbf{M}_S \begin{bmatrix} \ddot{Y} \\ \ddot{u} \end{bmatrix} + \begin{bmatrix} 2 \zeta \Omega & 0 \\ 0 & 2 \zeta_A \omega_A \end{bmatrix} \begin{bmatrix} \dot{Y} \\ \dot{u} \end{bmatrix} + \begin{bmatrix} \Omega^2 & \mu \bar{\kappa} \psi g / e \\ \kappa \psi g / e & \omega_A^2 \end{bmatrix}_{x=\xi} \begin{bmatrix} Y \\ u \end{bmatrix} = \begin{bmatrix} F(t)/M \\ 0 \end{bmatrix}, \quad (57)$$

$$\mathbf{M}_S = \begin{bmatrix} 1 + \mu \left\{ \phi^2 + \chi^2 + (\psi \mathrm{d}_A / e)^2 \left[1 + \bar{\kappa}_3' (H/\mathrm{d}_A)^2 \right] - 2 \chi \psi \mathrm{d}_A / e \right\} & \mu \left[-\bar{\kappa} \chi + (\bar{\kappa}_1 B + 2 \bar{\kappa} \mathrm{d}_A) \psi / 2e \right] \\ -\kappa \chi + (\kappa_1 B + 2 \kappa \mathrm{d}_A) \psi / 2e & 1 \end{bmatrix}_{x=\xi},$$

$$\mu = m_f e^2 / I_e. \quad (58)$$

Equations (57) and (58) turn out to be similar to the properly generalized modal Eq. (23), however, with force excitation understood.

5.1 Den Hartog tuning in case of dominating horizontal lateral bridge vibrations

In that case, the center of velocity falls (far) outside of the cross-sectional area at station $x = \xi$. Consequently both the vertical ϕ and torsional ψ mode shapes are set equal to zero in Eqs. (57) and (58). The mass ratio of the equivalent TMD results, cf. Eq. (30), and the optimal frequency ratio of the TLCGD changes accordingly to, cf. Eqs. (30) and (31),

$$\mu^* = \frac{m_A^*}{M^*} = \mu \left. \frac{\kappa \bar{\kappa} \chi^2}{1 + \mu \chi^2 (1 - \kappa \bar{\kappa})} \right|_{x=\xi}, \quad \mu = \frac{m_f e^2}{I_e} \quad (59)$$

and

$$\delta_{\text{opt}} = \frac{\omega_A}{\Omega} = \left. \frac{\delta_{\text{opt}}^*}{\sqrt{1 + \mu \chi^2 (1 - \kappa \bar{\kappa})}} \right|_{x=\xi}, \quad \zeta_{A,\text{opt}} = \zeta_{A,\text{opt}}^*. \quad (60)$$

Parametric excitation of the TLCGD by the vertical flexural vibrations of the bridge remains ineffective if the optimal linear damping coefficient is larger than the cut-off value of the most severe (double frequency) time-harmonic parametric resonance, [7]

$$\zeta_{A,\,\mathrm{opt}} = (4/3\pi)\,\delta_L \max|u| > \zeta_{A,\,0}^{(w)} = \kappa_1 \max|w\,(x=\xi_k)|/H. \tag{61}$$

5.2 Den Hartog tuning in case of dominating torsional bridge vibrations

The center of velocity lies inside of the cross-sectional area at station $x = \xi$. Consequently, the oblique flexural vibrations are neglected by putting both the vertical φ and lateral χ mode shapes equal to zero in Eqs. (57) and (58). The mass ratio of the equivalent TMD turns out in a more elaborate fashion, Eq. (62), with the optimal frequency ratio properly transformed,

$$\mu^* = \left.\frac{\mu(\bar\kappa_1 + 2\bar\kappa \mathrm{d}_A/B)\;(\kappa_1 + 2\kappa \mathrm{d}_A/B)\;\psi^2\,(B/2e)^2}{1+\mu\left[(\mathrm{d}_A/B)^2 + \bar\kappa_3'\,(H/B)^2 - (\bar\kappa_1 + 2\bar\kappa \mathrm{d}_A/B)\;(\kappa_1 + 2\kappa \mathrm{d}_A/B)/4\right](\psi B/e)^2}\right|_{x=\xi}, \tag{62}$$

$$\delta_{\mathrm{opt}} = \left.\frac{\delta^*_{\mathrm{opt}}}{\sqrt{1+\mu\left[(\mathrm{d}_A/B)^2 + \bar\kappa_3'\,(H/B)^2 - (\bar\kappa_1 + 2\bar\kappa \mathrm{d}_A/B)\;(\kappa_1 + 2\kappa \mathrm{d}_A/B)/4\right](\psi B/e)^2}}\right|_{x=\xi}. \tag{63}$$

The optimal damping coefficient, e.g., given in Eq. (32), remains unaffected. Parametric resonance in the torsional mode ($\ddot w = 0$ in Eq. (49)) remains ineffective if the sufficient condition applies—note the cut-off value of parametric resonance turns out differently to that given in Eq. (61), see again Fig. 7 and consider Eq. (50), [7],

$$\zeta_{A,\mathrm{opt}} = (4/3\pi)\,\delta_L \max|u| > \zeta_{A,0}^{(\vartheta)} = |\kappa_1 d_A/H - \kappa_2|\;\;\vartheta_{0,\max}^2/8. \tag{64}$$

5.3 Application of the TLCGD during the cantilever method of bridge construction

Wind gusts are critically forcing horizontal vibrations of the cantilevered bridge in construction, and consequently, the length of the cantilever must be limited. Stepwise tuning during the advancing construction length of the tip-positioned TLCGD increases the effective structural damping and thus allows much longer overhangs. A scaled model tested in the laboratory of the Author in the Institute of Building Construction and Technology, Fig. 8, convincingly approves the simulation results in both cases, under time harmonic contactless excitation, Fig. 9, where measured and numerically simulated dynamic magnification factors are shown to be in good agreement in the critical frequency window and further, by the forced decay rate of free vibrations, Fig. 10. The TLCGD is optimally tuned with respect to the basic mode of the cantilevered bridge [28].

6 The vertically acting tuned liquid column-gas damper

Earlier we have exemplarily shown that the U- or V-shaped tuned liquid column-gas damper (TLCGD) increases the effective structural damping of horizontal vibrations nearly as effective as an equivalent TMD with the additional advantage of easy frequency tuning by adjusting the gas equilibrium pressure. The novel pipe-in-pipe VTLCGD, sketched in Fig. 11, mitigates vertical vibrations, likewise to the spring-mass-dashpot TMD, [10]. Since one air chamber must be sealed for the sake of the required static over-pressure, the gas-spring effect is inherent in this design. The geometric analogy between the redesigned VTLCGD and the TMD still exists, making the first step in the tuning procedure 'classical'. Subsequently performed fine-tuning in state space of the VTLCGD, e.g., in the case when it is converted into smaller units in parallel action, renders an even more robust passive action, [11]. The experimentally observed averaged turbulent damping of the relative fluid flow and the weakly nonlinear gas-spring render the VTLCGD insensitive to overloads and, as well, to the parametric forcing caused by the vertical motion.

When considering a single-degree-of-freedom (SDOF-) main system, mass M_S, excited by vertical base acceleration and forced by $F(t)$, with such an alternative VTLCGD attached, see again Fig. 11, renders, upon

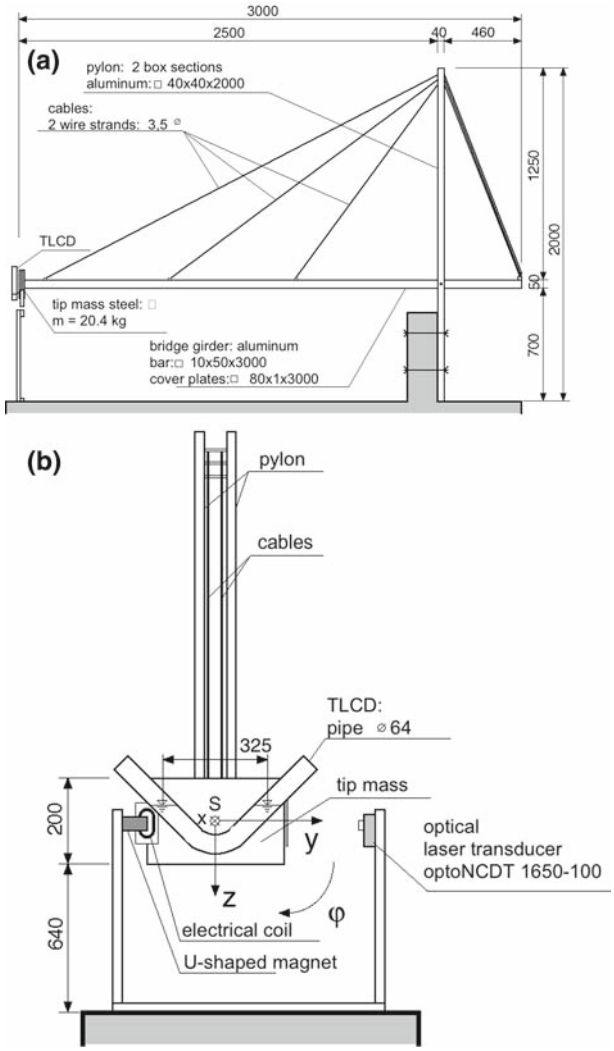

Fig. 8 Lab-model: cantilever method of bridge construction, dimensions in mm. **a** In side-view-**b** In front view, V-shaped TLCGD and electro-magnetic excitation shown, [28]

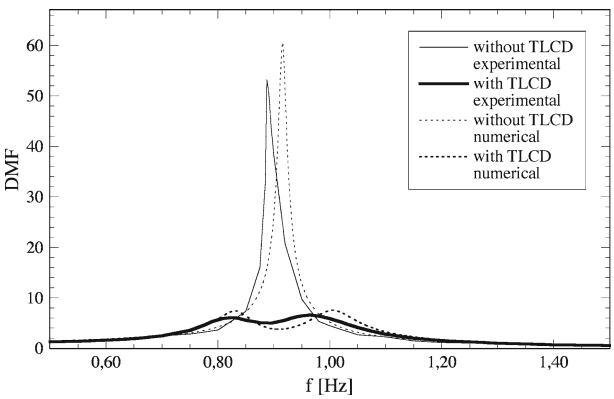

Fig. 9 Measured and simulated dynamic magnification factor of the horizontal tip-deflection in the critical frequency window, [28]

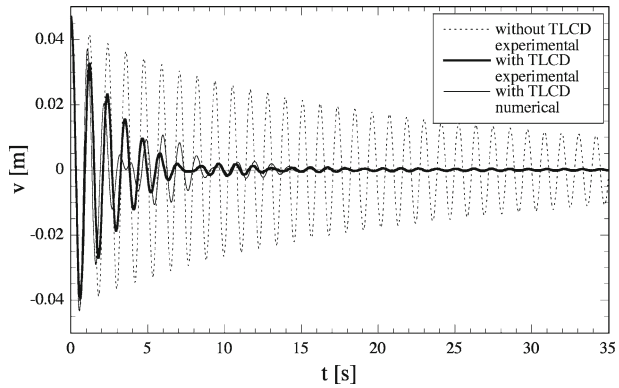

Fig. 10 Decay of free vibrations of the cantilevered bridge model, TLCGD optimized, [28]

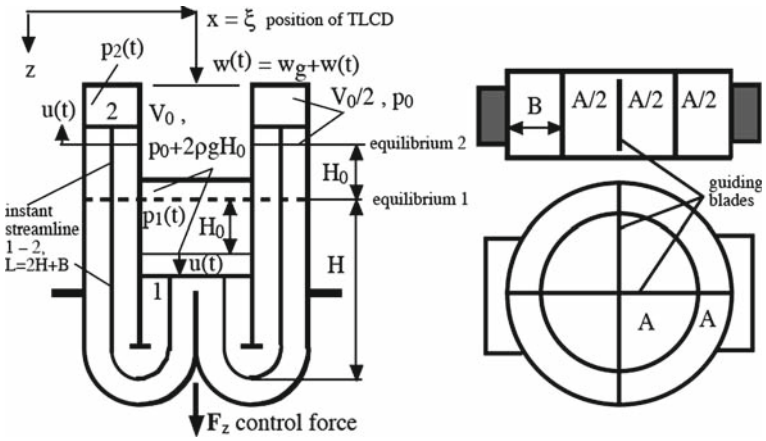

Fig. 11 Novel symmetric design of VTLCGD for vertical vibration damping, with flat or curved bottom, [10]. $B/H \ll 1$. The earlier design, [29], is improved. Static over-pressure head H_0 indicated in the "equilibrium 2" position. A circular cylindrical (axi-symmetric) design of the tank needs additional vertical, flat guiding blades to circumvent rotational flow

equivalent linearization of the turbulent damping $\delta_L \dot{u}\,|\dot{u}|$, resulting in the relation $\delta_L = \zeta_A 3\pi/4 \max|u|$, and after substitution of the first, linear part of the control force $F_z = F_1 + F_2$, the approximated coupled system of equations of motion

$$\begin{bmatrix} 1+\mu & -\mu\,\kappa_0 \\ -\kappa_0 & 1 \end{bmatrix} \begin{bmatrix} \ddot{w} \\ \ddot{u} \end{bmatrix} + \begin{bmatrix} 2\,\zeta_S\,\Omega_S & 0 \\ 0 & 2\,\zeta_A\omega_A \end{bmatrix} \begin{bmatrix} \dot{w} \\ \dot{u} \end{bmatrix} + \begin{bmatrix} \Omega_S^2 & 0 \\ 0 & \omega_A^2 \end{bmatrix} \begin{bmatrix} w \\ u \end{bmatrix} = -\begin{bmatrix} 1+\mu \\ -\kappa_0 \end{bmatrix} \ddot{w}_g + \begin{bmatrix} \frac{F(t)}{M} \\ 0 \end{bmatrix},$$

$$\mu = m_F/M_S, \tag{65}$$

$$\kappa_0 = 2H_0/L, \quad f_A = \frac{\omega_A}{2\pi} = \frac{\sqrt{\left(g/\pi^2\right)\left[1+(h_0+nH_0)/H_a\right]}}{\sqrt{4\,(L/2)}}, \quad F_1 = m_f\,\left(\ddot{w}_g + \ddot{w} - \kappa_0\,\ddot{u},\right),$$

$$F_2 = -m_f\,\left[u\,\ddot{u} + \dot{u}^2\right]/(L/2). \tag{66}$$

Note that, similarities exist to the more general Eq. (57) and compare the expression for the natural absorber frequency with that given in Eq. (10) for the TLCGD. Since the area of the cross-section of the VTLCGD is constant, $L_{\text{eff}} = L_1 = L = 2H + B$. Confer Eq. (22) as well. The parametric forcing term in the second of Eq. (65): $-\left[\left(\ddot{w}_g + \ddot{w}\right) u/(L/2)\right]$, has been omitted with sufficient damping understood. The cut-off value in this case is given by, [10,11],

$$\zeta_A > \zeta_{A,0}^{(w)} = \max\left|w_g + w\right|/(L/2) \ll 1. \tag{67}$$

Equation (65) is well suited for comparison with that of an equivalent TMD attached to the properly altered main SDOF-system, where an asterisk denotes all the relevant parameters. Den Hartog tuning, Eq. (32), of the

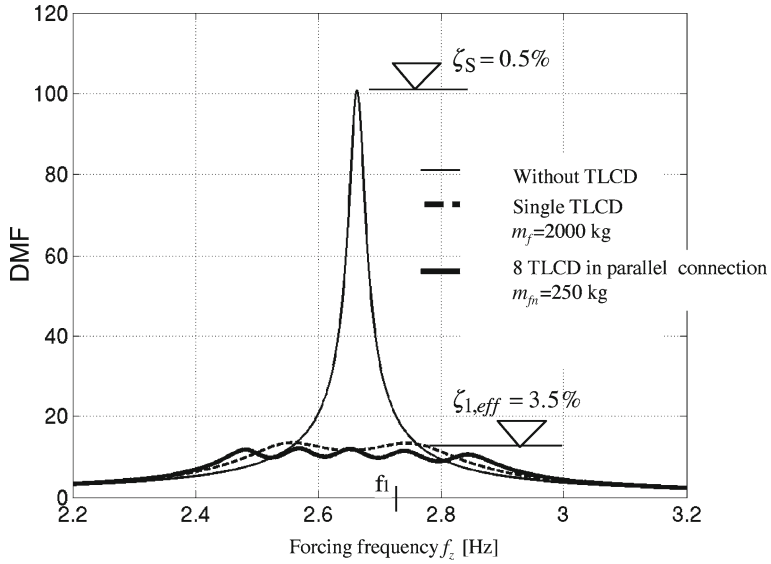

Fig. 12 Dynamic magnification factor of the vertical deflection at mid-span of a standard 50 m-span, SS-steel bridge in the critical frequency window around the first mode. Force excitation, $w_{stat} = F_0/k_1 = 0.95$mm. Single VTLCGD, and alternatively eight smaller units at mid-span, [10,30]

VTLCGD by analogy is made possible by the equivalent mass ratio, identified by inspection of the two systems of equations of motion, cf. Eq. (30) with $\kappa\bar{\kappa} \to \kappa_0^2$ substituted, as expected for a constant pipe cross-section,

$$\mu^* = m_A^*/M_S^* = \mu\kappa_0^2/\left[1 + \mu\left(1 - \kappa_0^2\right)\right]. \tag{68}$$

The formula remains applicable for modal tuning if the normal mode is normalized to one at the position of the VTLCGD, cf. to the more complex Eq. (30). The optimal frequency ratio is simply given by the transformation, cf. Eq. (31) for the more general case,

$$\delta_{\text{opt}} = f_{A\text{opt}}/f_S = \delta_{\text{opt}}^* \Big/ \sqrt{1 + \mu\left(1 - \kappa_0^2\right)}, \quad \zeta_{A\text{opt}} = \zeta_{A\text{opt}}^*. \tag{69}$$

The optimal linear damping coefficient, Eq. (32), is not affected by the transformation.

Equation (65) takes on a hyper matrix form for a multiple-degree-of-freedom main system with modal coordinates $Y_i, i = 1, 2, \ldots N$, with several VTLCGDs attached at properly selected positions $x = \xi_k, k = 1, 2, \ldots \text{r} \ll N$, and possibly converted into n_k smaller units in parallel action at one and the same location. In such a case, fine-tuning in state space is again recommended. The Den Hartog optimal parameters serve as initial values, e.g., in the standard program *fminsearch* of MATLAB [26].

The result of a numerical simulation within the critical frequency window of the basic mode, Fig. 12, of a single span, simply supported steel bridge of span 50 meters, modal mass $m_j = m\,l/2 = 35.72 \times 10^3$ kg, time-harmonically forced at mid-span, convincingly approve the damping effect even of a single, modally tuned VTLCGD with $m_f = 2{,}000$ kg, and further illustrates the increase of robustness of the damper when converted into eight smaller units in parallel action, all positioned at mid-span, [10,30]. The pressure in equilibrium1 state is prescribed, $p_0 = 1.2 \times 10^5$ Pa, and the surplus pressure head $H_0 = 0.70$ m is chosen in the equilibrium2 state. The optimal Den Hartog parameters of the single VTLCGD are derived following the two steps: (i) $\kappa_0 = 2H_0/L = 0.40$ is substituted in Eq. (68) to render the mass-ratio of the equivalent TMD, $\mu^* = 0.9\%$. (ii) When considering the result of Eq. (32) in Eq. (69), the optimal parameters turn out $f_{A1\,\text{opt}} = 2.64$ Hz and $\zeta_{A1\,\text{opt}} = 5.6\,\%$.

By means of the linear frequency of the equivalent mathematical pendulum and Eq. (66), Eq. (11) changes accordingly to render the altered design formula

$$(h_0 + nH_0)/H_a = L/2L_0 - 1. \tag{70}$$

Putting $n = 1.4$ yields for the assigned natural frequency the height of the gas volume $H_a = 0.380$ m, Eq. (70). The cross-sectional area $A = 0.571$ m^2 thus completes the design of the single VTLCGD. The maximum fluid stroke is linearly estimated to be max $|u| = 0.05$ m and thus is compatible within the design dimensions.

The most severe parametric resonance at double frequency must be considered, [7]. The deflection $\max|w(f_z = 2f_A)| = 10^{-3}$m results and, when substituted in the inequality (67) with $w_g = 0$, renders $\zeta_{A1\,\mathrm{opt}} = 5.6\% > \zeta_{A,0}^{(w)} = 0.08\%$, i.e., parametric forcing is fully negligible.

When considering four pairs of smaller VTLCGD units in parallel action, fine-tuning in state space requires the equilibrium1 gas pressure properly adjusted and, since the optimal damping of the fluid motion is much lowered, the maximum stroke is nearly doubled: $f_{A1,8,\mathrm{opt}} = 2.80$, $\zeta_{A1,8,\mathrm{opt}} = 1.85$, $f_{A2,7,\mathrm{opt}} = 2.51$, $\zeta_{A2,7,\mathrm{opt}} = 1.73$ and $f_{A3,8,\mathrm{opt}} = 2.61$ Hz, $\zeta_{A3,8,\mathrm{opt}} = 1.73\%$. The control becomes more robust as the inspection of Fig. 12 reveals. Since the maximum relative fluid speed still remains rather small, namely 1.7 m/s, no problems with respect to the application of the piston theory (intact fluid-gas-interface) are encountered, [12]. The inequality (67) still holds true.

7 Conclusions

The U- or V-shaped tuned liquid column damper substitutes equivalently the tuned mechanical damper if the vibration is dominantly horizontal, which occurs, e.g., either if the main system is a moderately asymmetric space frame, or if the main system is a bridge with critical lateral flexural-torsional natural modes, as made evident in this paper. For strongly asymmetric space frames (the definition is given in the paper), where rotation about the vertical axis dominates a (low frequency) natural mode, the special design of a torsional tuned liquid column damper turns out to be in fact more efficient in dissipating energy.

In both cases of (classical) TLCD and TTLCD, the size effect limits the application to extremely low frequencies in fractions of one Hertz. It is shown that the gas-spring effect in sealed dampers, like TLCGD/TTLCGD, not only extends the frequency range of application but also renders an easily accessible tuning parameter, namely the static equilibrium gas pressure in the symmetrically arranged gas containers above the upright pipe sections. In order to keep the fluid-gas interface intact, the allowable relative speed of the fluid must be limited as derived recently by *Wilhelm Schneider* and his research group. Consequently, it is pointed out that for a maximum given fluid stroke the frequency range of application becomes equally limited. A novel design of a VTLCGD is analyzed, which mitigates dominating vertical vibrations, e.g., of bridges and large floor-plates. In that case, at least a one-sided upright pipe section must be sealed to allow for a surplus of static pressure. For all these generalized tuned liquid column dampers an analogy is worked out to the equivalent mechanical dampers allowing modal tuning in an easy manner. Simple, case adapted transformations of the well documented optimization parameters of the TMD result and are presented in detail in the paper, yielding the desired frequency ratio but leaving the linear damping coefficient untouched. Hence, the widely used Den Hartog parameters apply as well. However, the sealed tuned liquid column dampers are insensitive to overloads and to the parametric forcing caused by any vertical or rotational motion due to the presence of both, the weakly nonlinear gas spring and the experimentally verified averaged turbulent damping. The latter is equivalently linearized in the course of the tuning process by analogy.

References

1. Petersen, Ch.: Schwingungsdämpfer im Ingenieurbau. Munich: Maurer S. 2001. ISBN 3-00-008059-7
2. Hochrainer, M.J.: Control of vibrations of civil engineering structures with special emphasis on tall buildings. Vienna University of Technology, Austria. http://www.tuwien.ac.at/. Dissertation 2001
3. Hochrainer, M.J.: Tuned liquid column damper for structural control. Acta Mech. **175**, 57–76 (2005)
4. Hochrainer, M.J., Ziegler, F.: Control of tall building vibrations by sealed tuned liquid column dampers. J. Struct. Control Health Monit. **13**(6), 980–1002 (2006)
5. Reiterer, M.: Damping of vibrational civil engineering structures with emphasis on bridges. Vienna University of Technology, Austria. http://www.tuwien.ac.at/. Dissertation, 2004
6. Reiterer, M., Ziegler, F.: Control of pedestrian-induced vibrations of long-span bridges. J. Struct. Control Health Monit. **13**(6), 1003–1027 (2006)
7. Reiterer, M., Ziegler, F.: Bi-axial seismic activation of civil engineering structures equipped with tuned liquid column dampers. J Seismol. Earthq. Eng. (JSEE) **6**(3), 45–60 (2004)
8. Fu, Chuan: Vibration control for asymmetric buildings. Vienna University of Technology, Austria. http://www.tuwien.ac.at/. Dissertation 2008
9. Ziegler, F., Fu, Chuan: Effective vibration damping of plan-asymmetric buildings. In: Sabouni, A.-R.R., El-Sawy, K.M. (eds.) The 8th Int. Conf. on Multi-Purpose High-rise Towers and Tall Buildings. The International Federation of High-Rise Structures, CD-ROM Paper ID IFHS-039. Abu Dhabi: 2007 (Download: http://www.acevents.ae "online documents" ifhs2007+ifhs2007dxb _TB-28.pdf) pp. 1–13

10. Reiterer, M., Ziegler, F.: Flüssigkeitstilger zur Tilgung von Schwingungen für Bauwerke. Patentschrift AT 501 870 B1, 2005-08-15, Österreichisches Patentamt. Patentanmelder: Vienna University of Technology, Austria, pp. 1–14
11. Ziegler, F.: Der Flüssigkeitstilger dämpft Schwingungen im Hoch- und Brückenbau. Bauingenieur **81**, 259–270 (2006)
12. Lindner-Silvester, T., Schneider, W.: The moving contact line with weak viscosity effects – an application and evaluation of Shikhmurzaev's model. Acta Mech. **176**, 245–258 (2005)
13. Lindner-Silvester, T.: Die bewegte Kontaktlinie mit schwachen Reibungseffekten. Vienna University of Technology, Austria. http://www.tuwien.ac.at/. Dissertation 2003
14. Zunzer, J.: Experimentelle und numerische Untersuchungen zur bewegten Kontaktlinie. Vienna University of Technology, Austria. http://www.tuwien.ac.at/. Dissertation 2002
15. Den Hartog, J.P.: Mechanical Vibrations Repr., 4th edn. McGraw-Hill, New York (1956)
16. Gao, H., Kwok, K.S.C., Samali, B.: Characteristics of multiple tuned liquid column dampers in suppressing structural vibration. Eng. Struct. **21**, 316–331 (1999)
17. Adam, C., Hruska, A., Kofler, M. : Elastic Structures with tuned liquid column dampers. In: Durakbasa, M.N., Afjehi, A., Osanna, P.H. (eds.) The XVI IMEKO WORLD CONGRESS, vol. VII, pp. 351–356. Intern. Measurement Confederation, Vienna (2000)
18. Chang, C.C., Hsu, C.T.: Control performance of liquid column vibration absorbers. Eng. Struct. **20**, 580–586 (1998)
19. Shum, K.M., Xu, Y.L.: Multiple-tuned liquid column dampers for torsional vibration control of structures: experimental investigation. Earthq. Eng. Struct. Dyn. **31**, 977–991 (2002)
20. Teramura, A., Yoshida, O.: Development of vibration control system using U-shaped water tank. In: 11th World Congress of Earthquake Engineering (WCEE, Sociedad Mexicana de Ingenieria Sismica, A.C.), paper ID-no. 1343. Elsevier Science Ltd (1996)
21. Huo, L.S., Li, H.N.: Torsionally coupled response control of offshore platform structures using circular tuned liquid column dampers. China Ocean Eng. **18**(2), 173–183 (2004)
22. Colwell, S., Base, B.: Tuned liquid column dampers in offshore wind turbines for structural control. Eng. Struct. (2008, in press)
23. Ziegler, F.: Mechanics of Solids and Fluids. Corr. Repr., 2nd edn. Springer, New York (1998)
24. Soong, T.T, Dargush, G.F.: Passive Energy Dissipation Systems in Structural Engineering. Wiley, Chichester (1997)
25. Warburton, G.B.: Optimum absorber parameters for various combinations of response and excitation parameters. Earthq. Eng. Struct. Dyn. **10**, 381–401 (1982)
26. MATLAB: User Guide, Control Toolbox. Version 6.5.1. MathWorks Inc. (2002)
27. Nowacki, W.: Baudynamik, Transl. 2nd Polish edn, (in German). Springer, Wien (1974)
28. Achs, G.: Anwendung von Flüssigkeitstilgern bei Schrägseilbrücken im Freivorbauzustand unter Windanregung. Diplomarbeit. Master Thesis, Vienna University of Technology, Austria. http://www.tuwien.ac.at/. Report: E206/3-No.1 (2005)
29. Sun, L.M., Nakaoka, I.: Tuned liquid damper for suppressing vertical vibrations. In: 45th JSCE Annual Meeting, vol. 1, pp. 978–979 (1990)
30. Ziegler, F.: The tuned liquid column damper as the cost-effective alternative of the mechanical damper in civil engineering structures. Int. J. Acoust. Vib. **12**(1), 25–39 (2007)